MULTIDISCIPLINARY OPTIMIZATION OF A NLF FORWARD SWEPT WING IN COMBINATION WITH AEROELASTIC TAILORING USING CFRP

DLR contribution to LuFo IV joint research project AeroStruct

T. Wunderlich, DLR Institute of Aerodynamics and Flow Technology, Braunschweig, Germany

S. Dähne, DLR Institute of Composite Structures and Adaptronic, Braunschweig, Germany

L. Heinrich, DLR Institute of Composite Structures and Adaptronic, Braunschweig, Germany

L. Reimer, DLR Institute of Aerodynamics and Flow Technology, Braunschweig, Germany

Abstract

This article introduces a process chain for commercial aircraft wing multidisciplinary optimization (MDO) based on high fidelity simulation methods. The architecture of this process chain enables two of the most promising future technologies in commercial aircraft design in the context of MDO. These technologies are natural laminar flow (NLF) and aeroelastic tailoring using carbon fiber reinforced plastics (CFRP). With this new approach the application of MDO to a NLF forward swept composite wing will be possible.

The main feature of the process chain is the hierarchical decomposition of the optimization problem into two levels. On the highest level the wing planform including twist and airfoil thickness distributions as well as the orthotropy direction of the composite structure will be optimized. The lower optimization level includes the wing box sizing for essential load cases considering the static aeroelastic deformations. Additionally, the airfoil shape adaptation based on sectional pressure distribution optimization and inverse design follows for the design point. Thereby, the objective function of the sectional pressure distribution optimization is the minimization of drag to find the best trade-off between profile drag considering NLF and transonic wave drag.

First optimization results of the multidisciplinary process chain are presented for a forward swept wing aircraft configuration. At this stage, airfoil shape optimization has not been included yet. Instead, natural laminar flow is considered by prescribing laminar-turbulent transition locations.

1 INTRODUCTION

The environmental impact of aviation increases with the rapid growth of air travel and transport. For this reason efficiency of future air transport must be improved significantly. The research and development of future transport aircraft have to meet this challenge. A Strategic Research Agenda has been developed by the "Advisory Council for Aeronautics Research in Europe" (ACARE). The goals of the European aeronautical research have been formulated in this research agenda and have been published in the "Vision 2020" [1], [2] and the "Flightpath 2050" [3]. In order to protect the environment and the energy supply a 50 % reduction of the CO_2 emissions per passenger kilometer has been requested for the year 2020 based on the values of the year 2000. The airframe contribution should be in the order of 20 % to 25 % in terms of fuel consumption reduction.

To achieve these challenging goals the development timescales for new technologies including new aircraft concepts have to be reduced significantly. For the assessment of an aircraft configuration it is essential to consider all relevant disciplines and their interactions on overall aircraft level. The consideration of new technologies and aircraft concepts requires a physics based approach because no statistics are available anymore. In order to represent the physics in a realistic manner, accurate simulation tools have to be applied. With increasing accuracy of the disciplinary simulations the geometrical description has to be improved too. This inherently leads to increased computational cost. The development of accurate and fast numerical simulation and optimization processes is getting more and more important. In this context new capabilities in the areas of process architecture, program interfaces, parallelization and the usage of high performance computing are required.

The combination of increasing computer resources and advanced numerical simulation tools enables the accurate prediction of flight performance of a transport aircraft configuration [4]. The use of these high fidelity simulation programs for aerodynamic design and optimization has been demonstrated in the MEGADESIGN project (Kroll et al. [5], [6], [7], [8] and Gauger [9]). State of the art high fidelity analysis methods already routinely include fluid-structure coupling of the aircraft wing for a given structural model. The consideration of fluid-structure interactions gets more important for the accurate performance and load prediction of highly flexible wings.

Improvements in automation and coupling of accurate simulation methods in combination with advances in numerical optimization strategies lead to the emergence of MDO based on high fidelity methods.

Multidisciplinary wing optimizations for realistic aircraft configurations under consideration of static aeroelasticity have been shown for example by Piperni et al. [10] for a large business jet and by Chiba et al. [11] for a regional jet.

The challenge in using MDO based on highly accurate methods is the large number of design parameters and the increased computational effort. To overcome this issue, the adjoint method enables the efficient calculation of the flow variable gradients as a function of the design parameters for gradient based optimizations. The adjoint method was used by Jameson, Leoviriyakit and Shankaran [12] for a gradient based multidisciplinary wing optimization with fluid-structure coupling. Up-to-date applications of the adjoint approach for multidisciplinary wing optimization have been shown in the publications of Kenway and Martins [13], Kenway, Kennedy and Martins [14] and Liem, Kenway and Martins [15]. These publications show that the gradient based optimization using the adjoint approach is an adequate method for multidisciplinary wing optimization with high fidelity simulation programs and a large number of design parameters.

In this article an alternative MDO approach is introduced for cases in which gradients cannot be computed efficiently for all relevant disciplines. This applies particularly to cases which involve laminar-turbulent transition prediction and structural sizing of composite structures using proprietary codes. Furthermore, a certain degree of flexibility in the process architecture and optimization strategy is desired. Especially the option to use optimization strategies seeking for the global optimum is important.

The application of MDO to new aircraft concepts and technologies using high fidelity methods is very promising. By using MDO an accurate comparison between optimal solutions based on conventional and new technologies will be possible. This facilitates an adequate assessment of new concepts and technologies on the one hand. On the other hand, this requires the availability of physics-based simulation models and efficient programs with adequate interfaces.

To improve the aerodynamic efficiency of commercial aircraft modern technologies for drag reduction have to be applied. A short overview of aerodynamic wing design and corresponding technologies is given for example by Horstmann and Streit [16]. One of the most promising drag reduction technology is laminar flow control (LFC). The potential of this technology for drag reduction of commercial aircraft has been described by Schrauf [17] and Green [18] for example.

In 1979, Boeing already investigated the benefit of NLF on large transport aircraft [19]. This study shows that the aircraft having a NLF wing design was not competitive against a turbulent wing design taking the top level aircraft requirements as a basis for comparison. In the DLR project LamAiR [20], however, the concept of forward sweep for laminar wings as proposed by Redeker and Wichmann [21] shows significant potential for efficiency improvements. In this project a multidisciplinary wing design of a forward swept wing having NLF and a composite structure including aeroelastic tailoring has been performed. The results are published by Kruse et al. [22].

The work on aeroelastic tailoring is summarized by Shirk et al. [23]. In this publication aeroelastic tailoring is described as *"...embodiment of directional stiffness into an aircraft structural design to control aeroelastic deformation, static or dynamic, in such a fashion as to affect the aerodynamic and structural performance of that aircraft in a beneficial way."*. Additionally, the advantages of composite materials on forward swept wings are explained. Tailoring the primary stiffness direction relative to the structural reference axis introduces a bend-twist-coupling that can be used to counteract the susceptibility of forward swept wings to static divergence. Dähne et al. [24] investigated the influence of aeroelastically tailored composites on structural mass. In the study an automated structural sizing process has been applied with the simplification that the aerodynamic loads remain fixed.

In striving for the capability to assess new wing technologies by development and application of a MDO process chain has been one of the main topics in DLR's contribution to the LuFo IV joint research project AeroStruct. In the scope of the project a process chain for multidisciplinary wing optimization considering new wing technologies such as forward sweep, NLF, composite materials and aeroelastic tailoring has been developed. In the setup of the process chain it was made sure that the aerodynamic loads of all load cases entering the structural sizing always result from fluid-structure coupled simulations. Wunderlich [25] showed that this has crucial influence on the multidisciplinary wing optimization results.

2 PROCESS CHAIN FOR MULTIDISCIPLINARY WING OPTIMIZATION

A process chain for multidisciplinary wing optimization based on high fidelity simulation methods has been developed. The developed process chain can be characterized by the following items:

- Usage of a central parametric file format,
- Automated grid generation for aerodynamic and structural analysis,
- Parallel and efficient aeroelastic analysis for j load cases,
- Structural wing box sizing for composite structures,
- Integration of inverse aerodynamic design for the design point and
- Consideration of NLF and aeroelastic tailoring.

The selected MDO architecture falls in the category of MDF-optimizations ("Multi-Disciplinary Feasible") and can be described as ASO ("Asymmetric Subspace Optimization") according to Martins and Lambe [26]. In the MDF architecture a full multidisciplinary analysis (MDA) is performed for each optimization iteration. This means that the investigated design in each optimization step fulfills all constraints and is called a feasible design.

In Fig. 1 the process chain is illustrated with a XDSM-diagram ("Extended Design Structure Matrix") [27]. This type of diagram combines the information of process flow between computational components with the information of data dependency. Each component in the diagram takes input data from the vertical direction and provides output data from the horizontal direction. "Data" is marked by rhombic shapes. Thick gray lines show the data flow. Thin black arrows indicate the process flow and a numbering system is used to define the order in which the components are executed.

The starting point for a multidisciplinary wing optimization is normally a detailed geometrical model of a given reference aircraft configuration. From this non-parametric model a fully parametric description of the aircraft using the common parametric aircraft configuration schema (CPACS) has to be generated manually or with a program in an automated way. Furthermore, the initial vector of design parameters $\vec{x}^{ini}$ is determined by the reference aircraft configuration. The load case definitions for the structural sizing have to be identified and stored in the CPACS dataset.

All disciplinary simulation programs in the process chain provide interfaces to this central hierarchical and human readable file format. In section 2.2 the parametric model and the CPACS dataset are described in more detail.

The driver component controls the optimization iteration and is represented in Fig. 1 by a rounded rectangle. Based upon a design parameter variation and a following transfer to the CPACS the disciplinary models are built or updated automatically. Thereby, the vector of design parameters $\vec{x}$ describes the wing planform including twist and airfoil thickness distributions and the orthotropy direction of the composite structure.

The static aeroelastic analysis is then run in parallel for all load cases including the design point under cruise flight conditions. For each load case the surface pressure distribution and aerodynamic coefficients of the wing are determined by solving the Reynolds-averaged Navier–Stokes equations (RANS) within a numerical flow simulation. Elastic characteristics of the wing and its internal load flows are determined using the finite element method (FEM). Subsequently, the wing mass is deduced by processing these internal loads. The interactions between the aerodynamic forces and the structural deformations of the elastic wing are taken into account in the aeroelastic analysis by loosely fluid-structure coupling as described in [28] and [29]. Thereby, the fluid-structure coupling loop stops when the values for the lift-to-drag ratio, wing mass and specific fuel consumption are converged.

Within the parallel aeroelastic analysis the wing box structure is sized and the bending- and torsional stiffness of the wing converge in the fluid-structure coupling loop. The main results of this parallel analysis are the wing mass m_W and the deformed wing shape for the design point under cruise flight conditions, which is normally called "1g-flight shape". Based on this 1g-flight shape and the corresponding lift distribution an automated target pressure generation and inverse design procedure follows.

The target pressure distribution for each selected wing section is designed for low drag considering the requirements for NLF. Thereby, constraints for local lift coefficient, pitching moment coefficient and airfoil thickness have to be fulfilled. An inverse aerodynamic wing design method is used for the transfer of these sectional target pressure distributions to the wing. The results of this inverse design procedure are the slightly changed airfoil shapes and the drag coefficient C_D for cruise flight conditions.

The last step in the process chain is the evaluation of the objective function f for the multidisciplinary assessment of the wing design. The optimization algorithm then calculates a new set of values for the design parameters based on the value of the objective function. After the optimization run has been finished the optimized vector of design parameters $\vec{x}^{opt}$ represents the main result of the process chain for the corresponding optimization problem.

2.1 Flight mission and objective function

For the evaluation of the objective function a simplified model of the flight mission has been used. This model is described in the textbook by Raymer [30] and is often used for preliminary aircraft design.

In this work, the flight mission consist of five segments. Table 1 gives an overview of these flight mission segments and the corresponding aircraft mass fractions. With the exception of the cruise flight segment the values for the aircraft mass fractions have to be prescribed depending on the optimization problem.

Segment number	Mission segment	Aircraft mass fraction
1	Warm-up and take-off	m_1/m_0
2	Climb and accelerate	m_2/m_1
3	Cruise	m_3/m_2
4	Descent for landing	m_4/m_3
5	Landing and taxi	m_5/m_4

Table 1: Flight mission segments and mass fractions.

For the cruise flight segment a constant flight speed V and a given constant lift coefficient C_L have been assumed. The flight speed V is determined by the selected design cruise Mach number Ma and the flight altitude H at the beginning of cruise flight. In combination with the assumption of constant thrust specific fuel consumption $TSFC$ this leads to

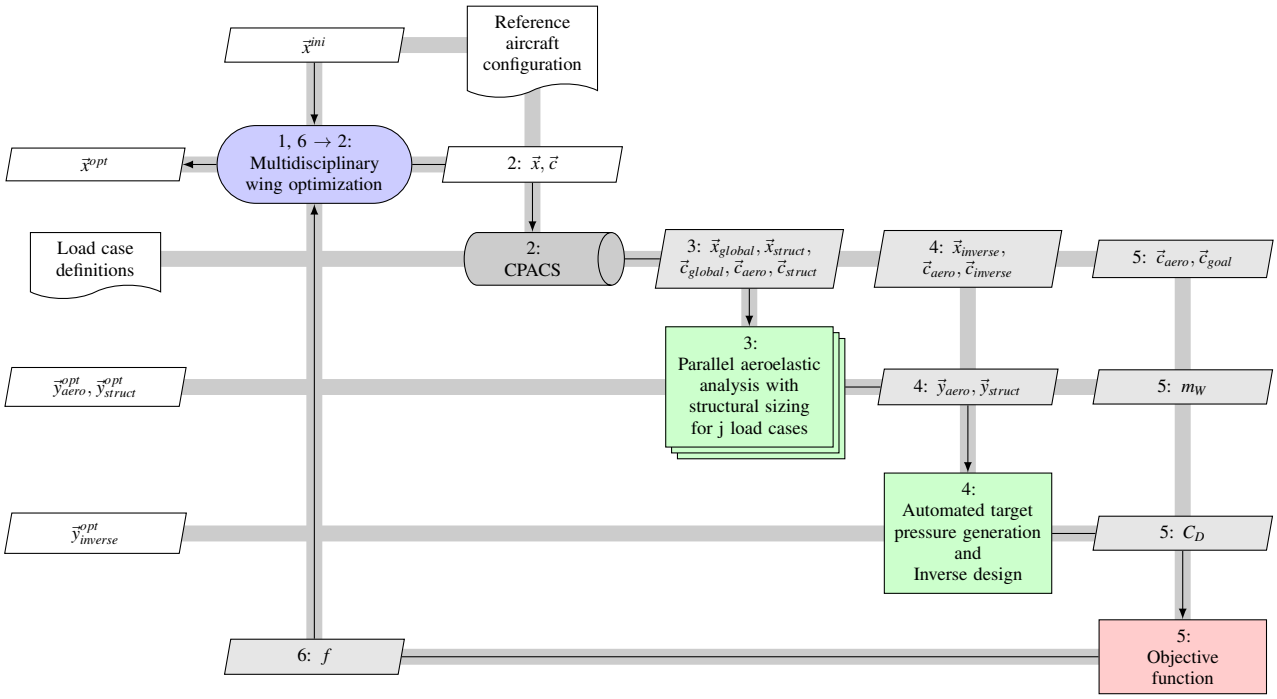

Figure 1: Flow chart of the process chain for multidisciplinary wing optimization.

the well known "Breguet range equation":

$$(1) \quad R = \frac{1}{g}\frac{V}{TSFC}\frac{L}{D}\ln\frac{m_2}{m_3}$$

The lift-to-drag ratio L/D of the aircraft for the given lift coefficient C_L and the wing mass m_W are results from the parallel aeroelastic analysis and the inverse design. Furthermore, the selected flight mission corresponds to the design mission. The outcome of this is that the aircraft mass m_0 at the start of the mission is equivalent to the maximum take-off mass m_{MTO}. For an aircraft the maximum take-off mass m_{MTO} is the sum of the residual mass m_{Res} (structural mass without the wing), the wing mass m_W, the payload m_P, the fuel mass m_F and the reserve fuel mass $m_{F,res}$:

$$(2) \quad m_{MTO} = m_{Res} + m_W + m_P + m_F + m_{F,res}$$

For the application of the process chain the maximum take-off mass m_{MTO} is held constant. Furthermore, the residual mass ratio m_{Res}/m_{MTO} is also assumed to be constant, because the optimization is limited to the wing. In accordance with the simple model for the flight mission the reserve fuel mass fraction $m_{F,res}/m_F$ is assumed to be constant as well.

The objective function f has to be selected based on the lift-to-drag ratio and the wing mass. Options for this selection are the minimization of fuel burn for a given range or the maximization of range for a given payload. Thereby, the objective function has to be derived for fixed maximum take-off mass.

For the transfer of the simulation results to the aircraft level the three following assumptions have been made.

Firstly, it has been assumed that the tailplane lift coefficient $C_{L,T}$ is constant. This means that the adaptation of tailplane lift for aircraft trimming has been neglected. The sum of wing- and fuselage lift coefficients $C_{L,W} + C_{L,F}$ results from the flow simulation and matches the prescribed target lift coefficient for the cruise flight.

Secondly, a constant sum of tailplane- and engine cowling drag coefficients (here denoted by $C_{D,res}$) has been assumed. The sum of wing- and fuselage drag coefficients $C_{D,W} + C_{D,F}$ is a result of the flow simulation and includes pressure and viscous parts. With these assumptions the aerodynamic performance in terms of lift-to-drag $L/D = C_L/C_D$ ratio is calculated with the following equation:

$$(3) \quad \frac{L}{D} = \frac{C_L}{C_D} = \frac{\overbrace{C_{L,W} + C_{L,F}}^{\text{flow simulation}} + \overbrace{C_{L,T}}^{=const.}}{\underbrace{C_{D,W} + C_{D,F}}_{\text{flow simulation}} + \underbrace{C_{D,T} + C_{D,E}}_{C_{D,res}=const.}}$$

Thirdly, the wing mass m_W is the sum of the wing box mass $m_{W,box}$ and the secondary wing masses $m_{W,sec}$. The secondary wing mass consist of the wing leading- and trailing edge masses, which have been prescribed in terms of mass per projected area. Additionally, the wing box mass is computed based on the sized finite element (FE) model and is multiplied by a correction factor of 1.25 to get a more realistic wing mass. This correction factor accounts for ad-

ditional structural mass, which is not modeled in the idealized wing box model.

2.2 Parametric model

For the parameterization of the aircraft the "Common Parametric Aircraft Configuration Scheme" (CPACS) [31] has been selected. This aircraft parameterization scheme uses the widely spread "Extensible Markup Language" (XML). Hence, the CPACS dataset represents a hierarchical organized and human readable file format.

The usage of CPACS offers a generic and fully parametric description of the aircraft. The geometrical description in CPACS is section based and developed for low-fidelity tools in conceptual design. For the usage in the context of high-fidelity simulation methods this geometrical description is not accurate enough. Therefore, some extensions have been introduced to the geometry description in CPACS through the definition of guide curves. These guide curves describe the surface geometry between the fuselage and wing sections respectively and will be used for the surface lofting. The resulting quality of the outer surface geometry is therefore appropriate for aerodynamic simulations with CFD methods.

In CPACS the inner geometry is defined based on the outer geometry description. This includes for example the parametric arrangement of spars, ribs and stringers. Also the used materials with their properties have to be defined in the CPACS dataset. The structural grid generation process is linked to the CPACS dataset and introduced in section 2.5.

Additionally, the definitions of operational cases and load cases for structural sizing are part of the CPACS dataset.

For the aerodynamic simulations a CAD model has been built automatically within the commercial software system CATIA® V5 based on the geometry description in CPACS. This parametric CAD model represents a direct copy of the geometrical description in CPACS with the same parametric description. The main task of the CAD model is the computation of the resulting surfaces and intersections for a given set of geometrical parameters in CPACS. In addition the CAD model includes the auxiliary geometry for the structured grid generation process.

2.3 Aerodynamic grid generation process

The automated CAD model generation in CATIA® includes the construction of the auxiliary geometry for the structured grid generation as mentioned before. Additionally, this CAD model generation program writes the control script for the structured aerodynamic grid generation using the commercial program Pointwise®.

In combination with the generated control script the extended CAD model forms the input for the automatic aerodynamic grid generation with Pointwise®. The control script includes all commands for the automatic generation of the structured aerodynamic grid.

This approach allows the fast and automatic grid generation for design parameter controlled geometrical changes within the optimization loop. Furthermore, the number of grid points is kept constant and the optimization process can be accelerated by using a fully converged flow solution as the starting point for solving the flow field around the modified aircraft geometry. With the usage of structured aerodynamic grids the grid dependent numerical noise is very low for geometrical changes, which is essential for accurate optimization results.

The actual implementation of the automated structured grid generation process is limited to the wing-fuselage configuration. But the introduced procedure is of general applicability to aerodynamic grid generation in the context of MDO.

2.4 Flow solver

The transonic flow around the wing-body aircraft configuration is simulated with the DLR TAU-code [32], [33], [34], which has been developed at the DLR Institute of Aerodynamics and Flow Technology. The TAU-code solves the compressible, three-dimensional Reynolds-averaged Navier–Stokes equations. It is a well established tool for aerodynamic applications at DLR, universities and aerospace industry [35], [36], [4]. The TAU-code uses a vertex centered dual mesh formulation. For spatial approximation, a finite volume method with second order upwind or central discretization is used.

For the flow simulation within the multidisciplinary process chain the central discretization schema and the Spalart–Allmaras turbulence model in the original version [37] has been used.

2.5 Structural grid generation process

For the generation of structure models, the software DELiS ("Design Environment for thin-walled Lightweight Structures") has been chosen. The core of DELiS is a parametric model generator that supports various levels of detail. Based on a CPACS dataset, DELiS creates an abstract, object oriented model of the aircraft. This model contains all the structurally relevant CPACS information and enriches it with required data for finite elements. Due to the abstract and FE-centric definition of the lightweight structure, models for various FE solvers can be created, such as MSC Nastran™ and ANSYS® [38].

In the scope of AeroStruct, two major enhancements to the automated model generation were implemented, namely the configuration-specific evaluation of fuel masses and secondary masses. As runtime plays an important role in predesign where numerous configurations have to be regarded, the aim in terms of efficiency was to consider load relief by fuel and secondary masses while keeping the overall model generation as fast as possible.

For the calculation of the fuel distribution, fuel tanks need to be defined in the dataset. Tank regions are based on references to existing ribs and spars. Together with a

maximum fill level, accounting for unusable volumes, components that are not modelled like pumps, fuel expansion reserves etc., the available volume can be calculated per rib bay and tank. In the next step, the fuel is then successively distributed to the tanks for each load case, whereby the outermost tank is filled first.

Leading and trailing edge high lift devices are not explicitly modelled. In order to consider their respective masses, a simplified approach has been chosen which is well established in predesign [39]. Semi-empirical values for these regions are taken from the literature in terms of mass per unit area. Based on these values and the projected areas of the individual configuration, the spanwise mass distribution is evaluated.

Fuel and high lift devices are modelled with point masses in the middle of corresponding rib bays. In Fig. 2, the FE representations of fuel and secondary masses are shown exemplarily. Fuel masses are converted to forces as they do vary between load cases. It should be mentioned, that rib positions are constant along the chord in this case but that is not necessarily the case.

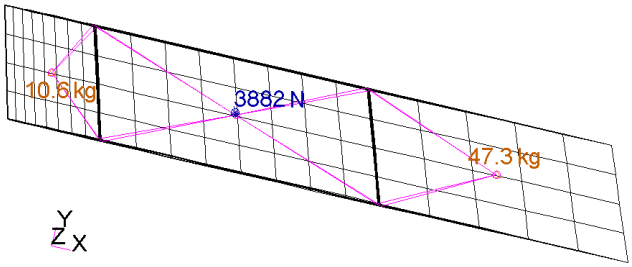

Figure 2: Rib bay with fuel and secondary masses.

2.6 Structural analysis and sizing

The aim of the structural sizing and optimization process is the minimization of the wing box mass $m_{W,box}$ with respect to a set of failure criteria. Thereby, all "Margins of Safety" (MoS) must be above MoS_{req}:

$$\begin{aligned} (4)\quad & \text{minimize} && m_{W,box}\left(\vec{x}_{struct}\right) \\ & \text{subject to} && \mathrm{MoS}_i\left(\vec{x}_{struct}\right) \geq \mathrm{MoS}_{req,i}\left(\vec{x}_{struct}\right) \end{aligned}$$

Based on the CPACS file an FE model of the wing is automatically generated as described in section 2.5. Rules for the discretization of the wing are implemented in the model generator to define optimization regions for wing cover, spars and each rib. With the external loads, which are calculated within the flow simulation and afterwards mapped on the FE model, the internal loads are calculated with linear-static FE calculations. Subsequently the FE model with its geometry, material properties and loads are passed to the sizing and optimization module.

In this module the geometry is post processed and components and assemblies are created. A component is an optimization region. In an assembly all components of the same part like the wing upper cover or the front spar are composed.

In a second step a design concept is assigned to each component. By considering the design concept only in the sizing and optimization module it is possible to investigate different design concepts with the same FE model because stiffeners are only considered explicitly during component sizing. As a result the creation of the FE model is simplified by smearing the stiffness of a stiffener into the overall panel stiffness and the stringers do not have to be modelled with discrete elements. Furthermore, an optimization of stringer profile and pitch is possible with the same model as well.

Failure criteria are also applied to the components, which serve as constraints for the optimization. Structure mechanical criteria for strength, damage tolerance, global buckling and local buckling can be used for the sizing of the components. Daehne et al. [24] have shown that global buckling, local buckling and strength are necessary failure criteria for reasonable results of mass and deformation. The failure criteria used for structural analysis are global buckling, local buckling and maximum strain for skin and stiffener. All criteria have been evaluated at ultimate load. Damage tolerance constraints have been covered by adapted strain allowables. For the strain allowable at ultimate load a conservative value of $3500^{\mu m}/_{m}$ has been chosen as proposed in military handbook [40]. Furthermore criteria from manufacturing and operations like minimum and maximum ply share in $0°/90°/+45°/-45°$ direction, minimum and maximum height for stringer webs and a minimum skin thickness for repair have been considered.

The component sizing itself is performed within a commercial software HyperSizer® [41]. The creation of components and assemblies as well as the assignment of the design concept and the failure criteria is done in HyperSizer®. An internal object model is created for each component. The object model contains all geometric parameter like stringer spacing, stringer height, skin thickness and web thickness. In addition, the material properties and failure criteria are also part of this object model.

The internal stresses are calculated from internal loads coming from the FE calculation and the stiffness of the panel objects. Due to the permutation based approach of HyperSizer® a great number of design candidates can appear which are reduced by an adaptive process based on the margin of safety. The resulting stiffness properties are evaluated by a further FE calculation. This process iterates until all failure criteria are fulfilled and the mass change is lower than the convergence threshold.

2.7 Fluid-structure coupling

The fluid-structure interaction loop to be carried out in every of the parallel aeroelastic analysis of Fig. 1 involves the following operations: (1) for every load case j, compute the

aerodynamic loads on the given CFD grid; (2) interpolate the loads from the CFD surface grid to the structural grid; (3) perform the structural sizing (once the loads of all load cases are available); (4) for every load case j, compute the structural deformations for the newly sized structure; and (5) adjust the CFD volume grid according to the resultant structural deformations. Then the loop starts over again. In step (2), an efficient classical nearest-neighbour interpolation is applied. It ensures equilibrium of forces on fluid and structural side. The existing defect in the equilibrium of moments is negligible. In step (5), a fast and robust grid deformation method is used which is based on the scattered data interpolation technology using radial basis functions. Based on the occurring structural deformations, a volume spline is determined which is then evaluated in parallel at all CFD volume grid points. Consult the publication by Barnewitz [42] for more detailed information on the grid deformation method.

The outlined fluid-structure interaction procedure is scripted in the FlowSimulator environment. The FlowSimulator has been designed particularly for massively-parallel multidisciplinary simulations with high-fidelity tools [43]. It is being jointly developed by Airbus, ONERA, DLR and universities. Its core, a C++ layer, provides parallel data containers and associated methods that support an efficient in-memory data exchange between involved process components. A Python scripting layer representing the users' level of access facilitates a fast creation of complex multidisciplinary process chains [44].

2.8 Automated target pressure generation

To optimize the airfoil shape for a given wing planform and lift distribution an automated target pressure generation combined with an inverse design method has been developed. This procedure allows the NLF wing design for transonic flight conditions and has been published by Streit et al. [45].

The automated target pressure generation process starts with the sectional pressure distributions for the cruise flight design point. For each selected wing section the pressure distribution is parameterized and then numerically optimized. The objective function of the pressure distribution optimization is the minimization of drag. This results in the best trade-off between profile drag considering NLF and transonic wave drag. Additionally, constraints for the lift coefficient, the pitching moment coefficient and the airfoil thickness have to be fulfilled. The pressure distribution optimization includes a boundary layer stability analysis using the e^N-method to predict the laminar-turbulent transition. Thereby, Tollmien-Schlichting- and crossflow instabilities are considered. Furthermore, the sectional conical wing approximation is integrated to model the three dimensional effects of swept and tapered wings.

For the transfer of the optimized sectional pressure distributions the inverse design method developed by Bartelheimer [46] is used. This method is based on the publication by Takanashi [47]. The automated target pressure generation and inverse design procedure is prepared for the integration into the process chain as shown in Fig. 1.

3 MULTIDISCIPLINARY WING PLANFORM OPTIMIZATION

The introduced process chain as described in section 2 has been used for the multidisciplinary wing planform optimization of a forward swept wing aircraft configuration. Thereby, the airfoil shape optimization with the automated target pressure generation and inverse design is not included. The laminar airfoils from the reference aircraft configuration have been used in the optimization. To consider the drag reduction of laminar flow the laminar-turbulent transition has been prescribed at a fixed percentage in chord direction. The goal of this optimization is to show first optimization results and demonstrate the applicability of the developed process chain. Some simplifications have been introduced to reduce the computational time.

3.1 Optimization problem description

3.1.1 Reference aircraft configuration

In the DLR project LamAiR [20] a multidisciplinary wing design of a forward swept wing with NLF and a composite structure including aeroelastic tailoring has been performed [22]. This aircraft configuration has been selected for the multidisciplinary wing optimization. Furthermore, the top level aircraft requirements and the design mission are identical to this aircraft configuration. The reference aircraft configuration has a low wing, rear mounted engines and a T-tail as shown in Fig. 3.

The selected reference aircraft configuration represents a short range commercial aircraft in the Airbus A320 class.

3.1.2 Design parameters and constraints

The selected design parameters for the wing planform optimization of the reference aircraft configuration are:

- Aspect ratio A,
- Leading edge sweep angle φ_{LE},
- Taper ratio λ.

The optimization constraints are listed in Tab. 2 and are based on the top level aircraft requirements and the results of the conceptual aircraft design published in [22]. This includes the specifications of the maximum take-off mass m_{MTO}, wing loading m_{MTO}/S and the cruise Mach number Ma.

For the structural sizing of the wing box three maneuver load cases with minimum and maximum load factors from the certification specifications CS-25/FAR 25 have been selected. The definitions of these selected load cases are specified in Tab. 3 and are based on the flight envelope of the reference aircraft configuration.

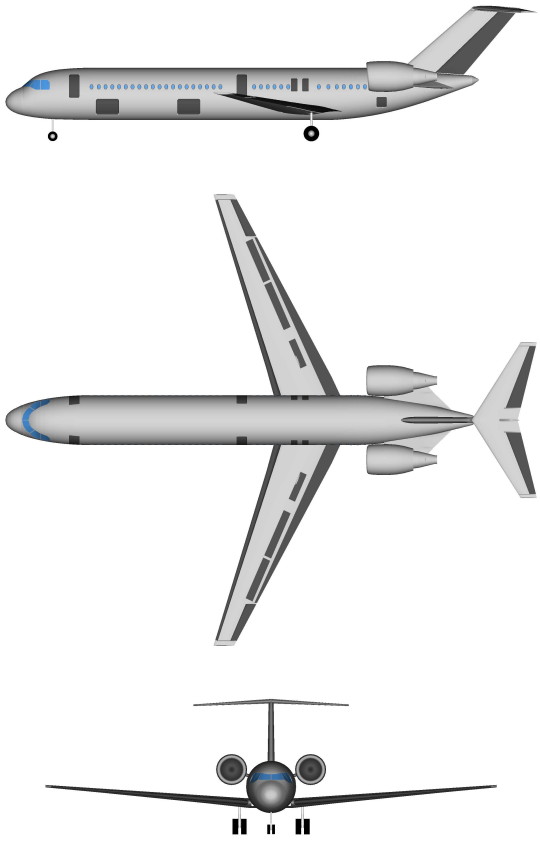

Figure 3: Reference aircraft configuration.

Aircraft		
Maximum take-off mass	m_{MTO}	73 365 kg
Wing loading	m_{MTO}/S	556 kg/m^2
Residual mass ratio	m_{Res}/m_{MTO}	0.4604
Drag coefficient of tailplane and engine cowling	$C_{D,res}$	0.0025
Specific mass of leading edge high lift device	m_{le}/S_{le}	30 kg/m^2
Specific mass of trailing edge high lift device	m_{te}/S_{te}	50 kg/m^2
Design mission		
Mach number	Ma	0.78
Range cruise segment	R	3726 km
Lift coefficient aircraft	C_L	0.5
Lift coefficient tailplane	$C_{L,T}$	-0.0022
Thrust specific fuel consumption	$TSFC$	0.0589 kg/(Nh)
Take-off and climb mass fraction	m_2/m_0	0.9589
Descent and landing mass fraction	m_5/m_3	0.9906
Reserve fuel mass fraction	$m_{F,res}/m_F$	0.4604

Table 2: Constraints of the wing planform optimization.

Load case	Altitude H	Mach number Ma	Lift coefficient $C_{L,W}+C_{L,F}$	Aircraft mass m	Load factor n
LC_2	0 m	0.597	0.539	73365 kg	2.5
LC_3	4725 m	0.772	0.571	73365 kg	2.5
LC_4	0 m	0.597	-0.216	73365 kg	-1.0

Table 3: Load cases for the structural sizing of the wing.

3.1.3 Objective function

Based on the simplified model for the flight mission as introduced in section 2.1 the specific fuel consumption SFC has been selected as the objective function for the multidisciplinary wing optimization. The specific fuel consumption SFC is here defined in terms of fuel burn per range and payload $m_F/(R\,m_P)$ for a given range R.

The minimization of the specific fuel burn is appropriate as a figure of merit for the multidisciplinary wing optimization of future commercial aircraft as shown in [48].

For the calculation of the specific fuel consumption the required equations are listed in Tab. 4. Thereby, the fuel mass m_F is computed from the given range R and the lift-to-drag ratio L/D. The payload m_P results from this fuel mass m_F and the wing mass m_W. With all these calculated values the fuel consumption per range and payload $m_F/(R\,m_P)$ follows directly from the last equation in Tab. 4.

Mass fraction cruise m_3/m_2	$\frac{m_3}{m_2} = e^{-\frac{g\,TSFC\,R}{V\,(L/D)}}$
Mass fraction fuel m_F/m_{MTO}	$\frac{m_F}{m_{MTO}} = 1-\frac{m_3}{m_2}\,\frac{m_1}{m_{MTO}}\,\frac{m_2}{m_1}\,\frac{m_4}{m_3}\,\frac{m_5}{m_4}$
Mass fraction payload m_P/m_{MTO}	$\frac{m_P}{m_{MTO}} = 1-\frac{m_{Res}}{m_{MTO}}-\frac{m_W}{m_{MTO}}-\left(1+\frac{m_{F,res}}{m_F}\right)\frac{m_F}{m_{MTO}}$
Specific fuel consumption SFC	$SFC = \frac{1}{R}\,\frac{m_F}{m_{MTO}}\,\frac{m_{MTO}}{m_P}$

Table 4: Equations for the calculation of fuel consumption.

3.2 Optimization results

The wing planform optimization has been performed successfully for the selected design parameters and constraints. In Tab. 5 the wing parameters resulting from the optimization are shown for the baseline and the optimized wing. The aspect ratio A and the absolute value of the leading edge sweep angle φ_{LE} of the optimized wing have been increased in comparison to the baseline wing. Furthermore, the taper ratio of the optimized wing is lower than the value of the baseline wing.

The optimization results for the lift-to-drag ratio, the wing mass ratio, the fuel mass ratio, the payload ratio and the specific fuel consumption are also given in Tab. 5. These results show an increased aerodynamic performance in terms of lift-to-drag ratio and simultaneously an increased wing mass for the optimized wing in comparison

		Baseline	Optimized
Aspect ratio	A	9.601	10.799
Leading edge sweep angle	φ_{LE}	$-16.8°$	$-19.7°$
Taper ratio	λ	0.345	0.172
Lift-to-drag ratio	L/D	19.02	20.16
Wing mass ratio	m_W/m_{MTO}	0.0999	0.1087
Fuel mass ratio	m_F/m_{MTO}	0.2119	0.2039
Payload ratio	m_P/m_{MTO}	0.2278	0.2269
Specific fuel consumption	SFC	$1.557 \cdot 10^{-4}\,\mathrm{km}^{-1}$	$1.504 \cdot 10^{-4}\,\mathrm{km}^{-1}$

Table 5: Results of wing planform optimization for baseline and optimized wing.

to the baseline wing. The increased lift-to-drag-ratio could be explained with the induced drag reduction resulting from the increased span and leads to the reduced fuel mass ratio. Only small differences in the payload ratio could be observed, because the reduced fuel mass almost compensates the increased wing mass. The main result of the wing planform optimization is the reduction of the specific fuel consumption SFC in the order of 3 %.

In Fig. 4 an overview of the wing planform optimization is given. This includes the comparison of the baseline and the optimized wing in terms of isentropic Mach number distribution for the upper wing, the deformations for the "2.5g-maneuver" and the "1g-cruise flight" and the corresponding lift distributions in span direction. Additionally, the prescribed laminar-turbulent transition line is shown in the isentropic Mach number distribution of Fig. 4. The relative position in chord direction has been held constant within the optimization.

The outboard load shift of both wings could be explained with the geometrical twist bending coupling of the forward swept wings and shows the importance of considering the static aeroelastic effects in the loads computation for the structural wing sizing.

4 CONCLUSION AND OUTLOOK

In the national joint research project AeroStruct a process chain for commercial aircraft wing MDO based on high fidelity simulation methods has been developed. This process chain enables the technologies NLF and aeroelastic tailoring using CFRP in the context of MDO.

The results for the multidisiciplinary optimization of a NLF forward swept composite wing show the influence of wing planform changes to the lift-to-drag ratio, the wing mass and the resulting fuel consumption. Thereby, the airfoil shape optimization is not yet included and the NLF is considered with a prescription of the laminar-turbulent transition. Furthermore, the efficiency and robustness of the parallel aeroelastic analysis including wing box sizing for three load cases has been successfully demonstrated.

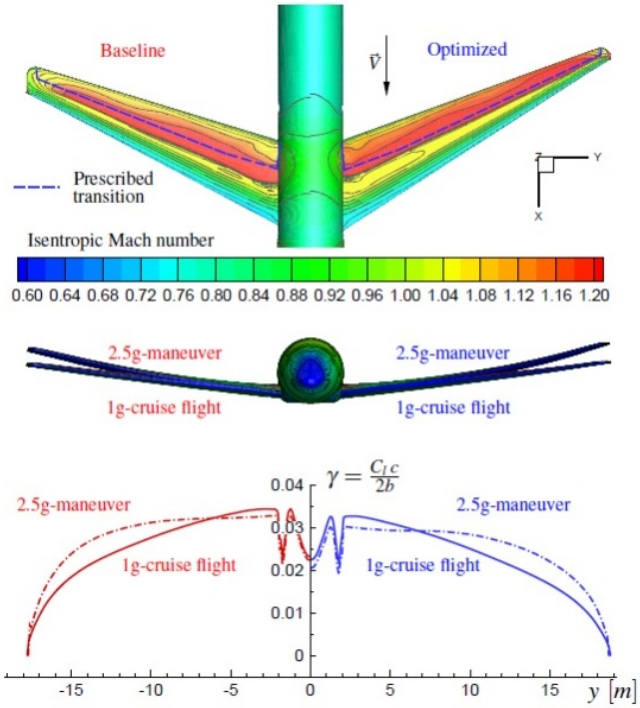

Figure 4: Overview of wing planform optimization.

The next step is the integration and validation of the automated target pressure generation and inverse design module in the process chain. Applications with the complete process chain for the MDO of the NLF forward swept composite wing with more design parameters are planned.

References

[1] European Commision. *European Aeronautics: A Vision for 2020*. Luxembourg, Belgium: Office for Official Publications of the European Communities, 2001.

[2] European Commision. *2008 Addendum to the Strategic Research Agenda*. http://www.acare4europe.com. 2008.

[3] European Commision. *Flightpath 2050 Europe's Vision for Aviation*. Luxembourg, Belgium: Office for Official Publications of the European Communities, 2011.

[4] N. Kroll et al. 'The MEGAFLOW-Project - Numerical Flow Simulation for Aircraft'. In: *Progress in Industrial Mathematics at ECMI 2004* (2005), pp. 3–33.

[5] N. Kroll et al. 'Ongoing Activities in Shape Optimization Within The German Project MEGADESIGN'. In: *ECCOMAS 2004*. 2004.

[6] N. Kroll et al. 'Flow Simulation and Shape Optimization For Aircraft Design'. In: *Journal of Computational and Applied Mathematics* 203 (Dec. 2005), pp. 397–411.

[7] N. Kroll et al. 'Ongoing Activities in Flow Simulation and Shape Optimization within the German Megadesign Project'. In: *ICAS 2006, 25th International Congress of the Aeronautical Sciences*. 2006.

[8] N. Kroll et al. *MEGADESIGN and MegaOpt - German Initiatives for Aerodynamic Simulation and Optimization in Aircraft Design*. Springer-Verlag Berlin Heidelberg, 2009.

[9] N. R. Gauger. 'Ongoing activities in shape optimization within the German project MEGADESIGN'. In: *EUCCO2004, Dresden (de), 29.-31.03.2004*. 2004.

[10] P. Piperni et al. 'Preliminary Aerostructural Optimization of a Large Business Jet'. In: *Journal of Aircraft* 44.5 (2007), pp. 1422–1438.

[11] K. Chiba et al. 'Multidisciplinary Design Optimization and Data Mining for Transonic Regional-Jet Wing'. In: *Journal of Aircraft* 44.4 (2007), pp. 1100–1112.

[12] A. Jameson et al. 'Multi-point Aero-Structural Optimization of Wings Including Planform Variations'. In: *45th Aerospace Sciences Meeting and Exhibit, Reno, Nevada, USA*. AIAA 2007-764. 2007.

[13] G. K. W. Kenway and J. R. R. A. Martins. 'Multi-point High-Fidelity Aerostructural Optimization of a Transport Aircraft Configuration'. In: 51 (2014). Journal of Aircraft, pp. 144–160.

[14] G. K. W. Kenway et al. 'Scalable parallel approach for high-fidelity steady-state aeroelastic analysis and adjoint derivative computations'. In: 52 (2014). AIAA Journal, pp. 935–951.

[15] R. P. Liem et al. 'Multi-point, multi-mission, high-fidelity aerostructural optimization of a long-range aircraft configuration'. In: *14th AIAA/ISSMO Multidisciplinary Analysis and Optimization Conference, Indianapolis, USA*. Sept. 2012.

[16] K. Horstmann and T. Streit. 'Aerodynamic Wing Design for Transport Aircraft - Today: Hermann Schlichting - 100 Years'. In: ed. by R. Radespiel et al. Vol. 102. Springer-Verlag Berlin Heidelberg, 2009, pp. 130–144.

[17] G. Schrauf. 'Status and perspectives of laminar flow'. In: *The Aeronautical Journal* 109.1102 (Dec. 2005), pp. 639–644.

[18] J. E. Green. 'Laminar Flow Control - Back to the Future?' In: *38th Fluid Dynamics Conference and Exhibit, Seattle, Washington, USA*. AIAA 2008-3728. 2008.

[19] G. W. Hanks et al. *Natural laminar flow analysis and trade studies*. Tech. rep. NASA CR-159029. National Aeronautics and Space Administration, 1979.

[20] A. Seitz et al. 'The DLR Project LamAiR: Design of a NLF Forward Swept Wing for Short and Medium Range Transport Application'. In: *29th AIAA Applied Aerodynamics Conference*. AIAA Conference Paper AIAA 2011-3526. June 2011.

[21] G. Redeker and G. Wichmann. 'Forward Sweep - A Favourable Concept for a Laminar Flow Wing'. In: *Journal of Aircraft* 28 (1991), pp. 97–103.

[22] M. Kruse et al. 'A Conceptual Study of a Transonic NLF Transport Aircraft with Forward Swept Wings'. In: *30th AIAA Applied Aerodynamics Conference, New Orleans, Louisiana*. AIAA Conference Paper AIAA 2012-3208. June 2012.

[23] M. H. Shirk et al. 'Aeroelastic tailoring - Theory, practice, and promise'. In: *Journal of Aircraft* 23.1 (1986), pp. 6–18.

[24] S. Dähne et al. 'Steps to Feasibility for Laminar Wing Design in a Multidisciplinary Environment'. In: *ICAS 2014*. Sept. 2014.

[25] T. F. Wunderlich. 'Multidisciplinary wing optimization of commercial aircraft with consideration of static aeroelasticity'. In: *CEAS Aeronautical Journal* 6.3 (2015), pp. 407–427.

[26] J. R. R. A. Martins and A. B. Lambe. 'Multidisciplinary Design Optimization: A Survey of Architectures'. In: *AIAA Journal* 51 (2013), pp. 2049–2075.

[27] A. B. Lambe and J. R. R. A. Martins. 'Extensions to the Design Structure Matrix for the Description of Multidisciplinary Design Analysis and Optimization Processes'. In: *Structural and Multidisciplinary Optimization* 46 (2012), pp. 273–284.

[28] R. Kamakoti and W. Shyy. 'Fluid-structure interaction for aeroelastic applications'. In: *Progress in Aerospace Sciences* 40.8 (2005), pp. 535–558.

[29] X. B. Lam et al. 'Coupled Aerostructural Design Optimization Using the Kriging Model and Integrated Multiobjective Optimization Algorithm'. In: *Journal of Optimization Theory and Applications* 142.3 (2009), pp. 533–556.

[30] D. P. Raymer. *Aircraft Design: A Conceptual Approach*. Third Edition. American Institute of Aeronautics and Astronautics, 1999.

[31] C. M. Liersch and M. Hepperle. 'A Unified Approach for Multidisciplinary Preliminary Aircraft Design'. In: *CEAS European Air and Space Conference, Manchester, United Kingdom*. 2009.

[32] M. Galle. *Ein Verfahren zur numerischen Simulation kompressibler, reibungsbehafteter Strömungen auf hybriden Netzen*. Tech. rep. DLR-Forschungsbericht 99-04. Braunschweig: DLR Institut für Aerodynamik und Strömungstechnik, 1999.

[33] T. Gerhold. 'Overview of the Hybrid RANS TAU-Code, In: Kroll N., Fassbender J. (Eds) MEGAFLOW - Numerical Flow Simulation Tool for Transport Aircraft Design'. In: *Notes on Multidisciplinary Design* 89 (2005).

[34] D. Schwamborn et al. 'The DLR TAU-Code: Recent Applications in Research and Industry'. In: *European Conference on Computational Fluid Dynamics, ECCOMAS CFD 2006 Conference, Delft, The Netherlands*. 2006.

[35] N. Kroll and J. K. Fassbender. 'MEGAFLOW - Numerical Flow Simulation for Aircraft Design, Braunschweig'. In: *Notes on Numerical Fluid Mechanics and Multidisciplinary Design (NNFM)* 89 (2002).

[36] N. Kroll et al. 'MEGAFLOW - A Numerical Flow Simulation Tool For Transport Aircraft Design, Toronto, Canada'. In: *ICAS Congress 2002*. 2002, pp. 1.105.1–1.105.20.

[37] P. R. Spalart and S. R. Allmaras. 'A one-equation turbulence model for aerodynamic flows'. In: *30th AIAA Aerospace Sciences Meeting and Exhibit*. AIAA-92-0439. 1992.

[38] S. Freund et al. 'Parametric Model Generation and Sizing of Lightweight Structures for a Multidisciplinary Design Process'. In: *NAFEMS Konferenz: "Berechnung und Simulation - Anwendungen, Entwicklungen, Trends*. May 2014.

[39] E. Torenbeek. *Synthesis of subsonic airplane design*. Delft: Delft University Press, 1976.

[40] M.-H.-1.-3. Military. *Composite Materials Handbook, Polymer Matrix Composites: Materials Usage, Design, and Analysis*. Vol. 3 of 5. US Department of Defense, June 2002.

[41] *HyperSizer Documentation*. Collier Research Corporation. Newport News, 2015.

[42] H. Barnewitz and B. Stickan. 'Improved Mesh Deformation'. In: *Notes on Numerical Fluid Mechanics and Multidisciplinary Design*. Ed. by B. Eisfeld et al. Vol. 122. 2013, pp. 219–243.

[43] M. Meinel and G. O. Einarsson. 'The FlowSimulator framework for massively parallel CFD applications'. In: *PARA 2010 conference, 6-9 June, Reykjavik, Iceland*. 2010.

[44] L. Reimer et al. 'Multidisciplinary Analysis Workflow with the FlowSimulator'. In: *Proceedings of the Onera Scientific Day 2012—CFD Workflow: Mesh, Solving, Visualizing, ...* Ed. by C. Benoit et al. Vol. 19. Amphithéâtre Becquerel, École Polytechnique, Palaiseau, 2012, pp. 23–30.

[45] T. Streit et al. 'DLR Natural and Hybrid Transonic Laminar Wing Design Incorporating New Methodologies'. In: *RAeS Advanced Aero Concepts, Design and Operations Conference*. July 2014.

[46] W. Bartelheimer. 'An inverse method for the design of transonic airfoils and wings'. In: *Inverse Problems in Engineering* 4 (1996), pp. 21–51.

[47] S. Takanashi. 'Iterative Three-Dimensional Transonic Wing Design Using Integral Equations'. In: *Journal of Aircraft* 22.8 (Aug. 1985), pp. 655–660.

[48] T. F. Wunderlich. 'Multidisziplinärer Entwurf und Optimierung von Flügeln für Verkehrsflugzeuge'. In: *Deutscher Luft- und Raumfahrtkongress, Aachen*. DGLR-Tagungsband - Ausgewählte Manuskripte DLRK2009-1181. Sept. 2009.